IAWA Journal, Vol. 28 (2), 2007: 189–209

WITHIN TREE VARIATION OF LIGNIN, EXTRACTIVES, AND MICROFIBRIL ANGLE COUPLED WITH THE THEORETICAL AND NEAR INFRARED MODELING OF MICROFIBRIL ANGLE

Brian K. Via[1,4], **Chi L. So**[1], **Leslie H. Groom**[2], **Todd F. Shupe**[1], **Michael Stine**[1] and **Jan Wikaira**[3]

SUMMARY

A theoretical model was built predicting the relationship between microfibril angle and lignin content at the Angstrom (Å) level. Both theoretical and statistical examination of experimental data supports a square root transformation of lignin to predict microfibril angle. The experimental material used came from 10 longleaf pine (*Pinus palustris*) trees. Klason lignin (n=70), microfibril angle (n=70), and extractives (n=100) were measured and reported at different ring numbers and heights. All three traits were strongly influenced by ring age from pith while microfibril angle and extractives exhibited more of a height effect than lignin. As such, the multivariate response of the three traits were different in the axial direction than the radial direction supporting that care needs to be taken when defining juvenile wood within the tree. The root mean square error of calibration (RMSEC) for microfibril angle of the theoretical model (RMSEC = 9.8) was almost as low as the least squares regression model (RMSEC = 9.35). Microfibril angle calibrations were also built from NIR absorbance and showed a strong likeness to theoretical and experimental models (RMSEC = 9.0). As a result, theoretical and experimental work provided evidence that lignin content played a significant role in how NIR absorbance relates to microfibril angle. Additionally, the large variation in extractives content coupled with sampling procedure proved important when developing NIR based calibration equations for lignin and microfibril angle.

Key words: NIR, polymer, lignin, extractives, microfibril angle, growth rate.

---

1) School of Renewable Natural Resources, Louisiana State University Agricultural Center, Baton Rouge, LA 70803, U.S.A.
2) USDA Forest Service, Southern Research Station, Pineville, LA 71360, U.S.A.
3) Department of Chemistry and Wood Technology Research Centre, University of Canterbury, Christchurch, New Zealand.
4) Current address: Louisiana Pacific R&D Technology Center, 308 Mallory Station Road, Franklin, TN 37067 [E-mail: brian.via@lpcorp.com].

Association Editor: Laurence Schimleck

INTRODUCTION

The composition and orientation of polymers in the cell wall change as a function of age and growth rate. Likewise, tracheid length changes with age and may be a function of polymer orientation in the primary wall. Polymer orientation may be an important factor determining cell length since the cellulosic matrix is formed perpendicular to the cellulose chain (Gunning & Hardham 1982). Similarly, development of the secondary wall (S_2 layer) during cell wall thickening occurs in the plane perpendicular to polymer orientation. In the S_2 layer, polymer alignment is less variable when compared to the primary wall with microfibrils showing a high degree of order from lamella to lamella.

When cell growth occurs in proximity to the apical meristem, auxin concentrations are high and will influence fiber dimensions (Brown 1970). For example, the addition of the hormone gibberellic acid (GA) results in increased tree growth (Gunning & Hardham 1982) and may influence microfibril angle and lignin content. A high microfibril angle and lignin content is needed to resist gravity and wind loads for young trees (Lichtenegger *et al.* 1999; Reiterer *et al.* 1999). Also, a high microfibril angle incorporates extensibility needed during wind loading while increased lignin adds stiffness resistance to compression forces (Hepworth & Vincent 1998; Köhler *et al.* 2000, Köhler & Spatz 2002).

With increased radial cell formation, a slower growth rate occurs over time. In turn, the S_2 microfibrils are oriented at a lower angle and lignin content commonly decreases as the tree matures (Larson 1966; Shupe *et al.* 1996a and 1996b, 1997). The correlation between lignin content and cellulose is quite high when isolated from just the S_2 layer and avoiding middle lamella formed lignin (Gindl & Teischinger 2002). Likewise, the relationship between lignin and microfibril angle is strong for 20 coniferous wood species (Saka & Tsuji 1987). Several investigators have reported an increase in lignin and microfibril angle with increased fertilization, irrigation, temperature, earlywood %, and thinning (Wardrop & Dadswell 1955; Erickson & Arima 1974; Shupe *et al.* 1996a, 1997; Lindström *et al.* 1998; Herman *et al.* 1999; Gindl *et al.* 2000; Wimmer *et al.* 2002; Sarén *et al.* 2004; Lundgren 2004). Microfibril angle, however, has been shown to decrease with tree height, density, and slower growth rate (McMillin 1973; Donaldson 1992; Evans *et al.* 2000). Indeed, the apparent relationship between growth, microfibril angle, and lignin is not passive. McCann *et al.* (1993) showed that cellulose deposition, and hence microfibril angle, dictates other polymer concentrations, spacing, and orientations. Taylor *et al.* (1992) found lignin deposition to vary locally with cellulose deposition within the secondary cell wall of tracheary elements. As well, the lignin distribution closely follows the microfibrils in the S_2 layer for *Picea abies* (Singh & Daniel 2001).

The ability to use absorbance in the near infrared range to estimate microfibril angle is receiving increasing attention in the scientific community. Such correlation between NIR absorbance and microfibril angle have been detected both across various ages and within specific density classes for radiata pine (*Pinus radiata*), loblolly pine (*Pinus taeda*), and eucalyptus (*Eucalyptus globulus*) (Schimleck *et al.* 2001; Schimleck &

Evans 2002; Schimleck *et al.* 2002; Schimleck *et al.* 2003a; Jones *et al.* 2005; Schimleck *et al.* 2005). On the other hand, the basis for how NIR can measure microfibril angle is still uncertain (Gindl *et al.* 2001). Wavelengths associated with cellulose have shown considerable variation in response to microfibril angle (Kelley *et al.* 2004a). Such a relation to cellulose associated wavelengths seems logical but presently only empirical equations have been developed. Since the summation of cellulose, hemicellulose, and lignin theoretically sum to >95 % of the total chemistry content in cell walls for extractive free wood, only one variable may be needed to account for the variation in microfibril angle since additional variables may be statistically redundant. But also, extractives content can be influential on the spectra, especially in the pith wood of *P. palustris* where extractives concentration is not negligible. As such, monitoring the extractives content or extraction prior to testing should improve the confidence during NIR model development.

Lignin content was predetermined to be the best candidate for microfibril angle prediction since lignin relates to microfibril angle and can easily be estimated from absorbance response in the NIR region (Gindl & Teischinger 2002; Baillères *et al.* 2002; Poke *et al.* 2004; Yeh *et al.* 2004). However, this is not to say that cellulose content does not also influence the spectra. For example, Jones *et al.* (2005) confer of the impact of microfibril angle on the absorbance of cellulose associated wavelengths. Future studies investigating cellulose content, as measured through wet lab chemistry, on microfibril angle would be useful. Nonetheless, development of a model to predict microfibril angle from lignin content is a good first step in explaining how NIR absorbance and microfibril angle co-vary. Such a relationship would be useful in plant science where both traits are known to influence plant and wood mechanical properties (Hoffmann *et al.* 2003).

The objectives of this paper was fourfold: 1) to develop near infrared models for lignin, extractives, and microfibril angle, 2) to measure the lignin, extractives content, and microfibril angle from pith to bark and breast height to tip, 3) to analyze the relationship between microfibril angle and extractive free lignin through empirical and theoretical means, 4) to compare theoretical and NIR spectroscopy models of microfibril angle with interpretation.

MATERIALS AND METHODS

Sample preparation

Ten longleaf pine (*Pinus palustris*) trees were harvested from the location 30.6° north and 89.1° west. Periodic fires were prescribed throughout the 41 years of the stand resulting in little competition from understory plants. Seedlings were spaced 3.7 m apart in a equilateral triangle pattern. Each tree was cross cut every 4.6 m in height, yielding 5 to 7 bolts and accompanying disks. The disk was always taken from the basal direction of the bolt. A 2 mm thick strip was cut from the disk such that the radial face was exposed for later NIR scanning. Likewise, a 10 mm wide strip was taken for microfibril angle measurement. The 10 mm wide strip was dissected by ring with the tangential face showing and a mean 1 mm thickness in the radial direction.

All specimens were allowed to equilibrate to room humidity and temperature. Microfibril angle samples were first air dried to room moisture content and then further dried in an oven at 105 °C. The remainder of the disk was used for chemical analysis.

The samples used for NIR calibration were also the same samples used to determine within tree variation. Likewise, the same samples used for NIR calibration of lignin and extractives were also used for NIR and theoretical modeling of microfibril angle.

Chemical analyses

The remainder of the disk was separated into latewood fractions for rings 4, 8, 16, and 32 from the pith for all heights of each tree. Therefore, the circumference of the disk was dissected into small slivers (≈1 to 3 mm thick by 10 mm long) of wood for each ring and height category. All slivers were milled using a Wiley mill and allowed to pass between a 40 to 60 mesh screen. All samples were analyzed for extractives and lignin by standard test methods (Tappi 1997, 1998). A replication of three was used for chemistry determination of all samples. Preliminary testing found the lignin content standard error (standard deviation around the mean) to be 0.4% within an average test run (n=5 per run) and 0.69% when all test runs were pooled (n=20). For extractives content, preliminary testing showed extractives content standard error to be 0.48% within an average test run (n=12 per run) and 1% when all test runs were pooled (n=60). A total of 70 samples were processed for lignin determination and a total of 100 samples were processed for extractives determination. These samples were used in the calibration of the near infrared instrument. The samples used for calibration of the NIR instrument were also 4, 8, 16, and 32. Ring 1 was not included in the calibration due to the lack of consistent material volume.

Microfibril angle measurements

Small molecule X-ray crystallography was performed on a Bruker diffractometer. The T-value, a value closely related to Evans' variance intensity of the (002) arc, was acquired in conjunction with the microfibril angle, a value also provided by Cave as estimated by the equation T = MFA+2*SDA where SDA represents the standard deviation of the flank angle (Cave 1966; Cave personal communication). A differential interference contrast (DIC) microscope was used to estimate the microfibril angle after fiber maceration for 48 hours. Other than the additional time to maceration, the procedure provided by Peter *et al.* (2003) was used. Nine samples ranging between 45 and 10 degrees microfibril angle were measured with a replicate of 30 fibers per sample to estimate the microfibril angle to a ± 2 degree standard error. The slope between the T-value and microfibril angle was statistically equivalent to the slopes estimated by the Cave equation throughout the T-value region, thus the Cave equation was used (1996). The R^2 for the calibration technique was 0.70. The X-ray beam was aimed such that it was parallel to the radial direction and passed through latewood having an average thickness of 1 mm. The sample width was parallel to the tangential surface and had a mean of 5 mm. The height was parallel to the axis of the tracheids and averaged 10 mm. A total of 70 latewood microfibril angle measurements were made on the same 70 latewood samples measured for lignin.

NIR Spectroscopy

The NIR absorbance measurements were obtained along the radial face strip using a Nexus 670 FT-IR spectrometer (Thermo Nicolet Instruments, Madison, WI, U.S.A.). Absorbance readings were acquired between 1000 to 2500 nm wavelengths. Forty scans were acquired at 1 nm intervals using reflectance spectroscopy and then averaged. The 1 nm intervals were next averaged into 10 nm intervals with no loss in spectral resolution (Schimleck *et al.* 2004). The spot size of the scanning area was 5 mm. The ring width was variable and was considerably smaller than the diameter of the spot size in the mature wood region; therefore, the latewood ring of interest was always placed in the center of the spot. Specifically, the combined latewood and earlywood width in the mature wood zone was always less than 2 mm while in the juvenile wood zone, the earlywood and latewood width was always greater than 5 mm. The samples were illuminated with a lamp source at approximately 30 degrees to the sample. A curtain was placed around the scanning area so as to minimize light differences between tests. A white Spectralon reference sample was scanned every 10 minutes to avoid any drift that might occur over time.

Calibration development

The loadings from principal components regression (SAS 2001) was used to determine which wavelengths were most important in predicting lignin, extractives, and microfibril angle. The wavelengths were then analyzed using stepwise regression to determine which wavelengths were significant in predicting the y variable ($\alpha = 0.10$) (SAS 2001). Coefficients and intercepts were then chosen and the model was developed for each trait. Cross validation was used to ensure stable calibration equations. Spectra pretreatments, such as derivatives or multiplicative scatter correction, was employed but was not used in calibration if the pretreatment did not provide a model with less error for a given number of factors.

For all NIR models, the origin of the model was derived through C_p model selection. The C_p model selection tool was used to determine the model with the most predictive power. The detailed procedure for this selection tool is outlined in Via *et al.* (2005) and the same procedure was used in this study.

THEORETICAL MODEL DEVELOPMENT

The presumption of the model developed herein is that a response to growth occurs in the lignin matrix perpendicular to the axis of the cellulose chain. Figures 1 & 2 show the cross section and longitudinal view of the microfibril model, respectively. When the microfibril angle equals 0 degrees (Fig. 2a), the growth required to reach the target plane is minimal. However, as the microfibril axis rotates, the growth needed to reach the target plane increases in a nonlinear manner (Fig. 2b). The growth is theorized to occur in the lignin sheath, which surrounds the microfibril (Fig. 1). The low lignin scenario corresponds with a low growth (G vector low) while high lignin content corresponds with increased growth. To simplify the model, variation in hemicellulose distances, between cellulose crystallites, was kept constant at 25 Å and the cellulose

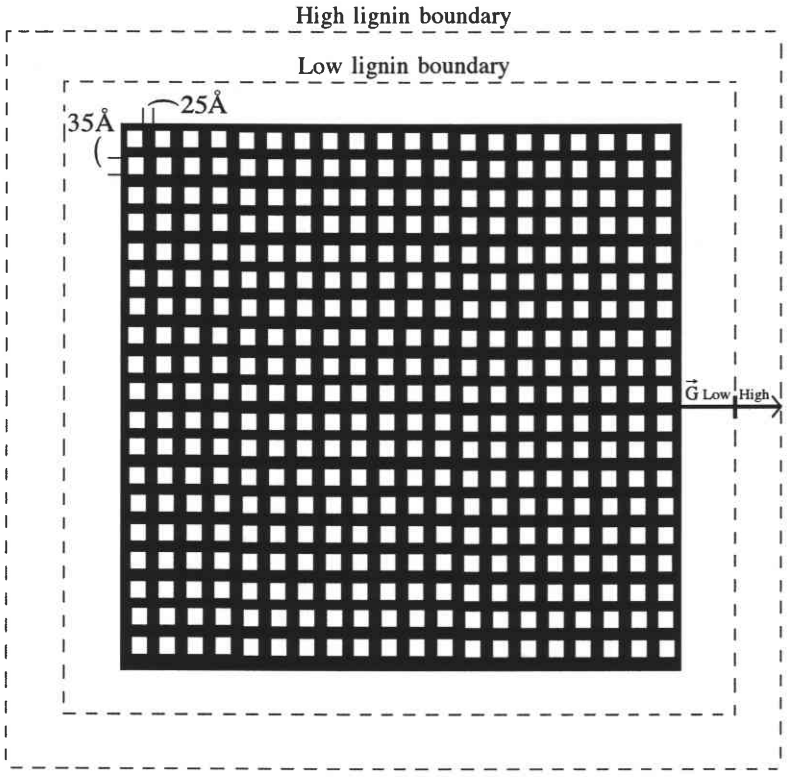

Figure 1. Cross section view of microfibril with cellulose elementary fibers in white, hemicellulosic matrix in black, and lignin acting as a sheath [simplified model and distances adapted after Heyn (1969), Nieduszy & Preston (1970), Fengel (1970), and Donaldson (2001)]. Note that the G_{low} and G_{high} represent the growth vector of lignin.

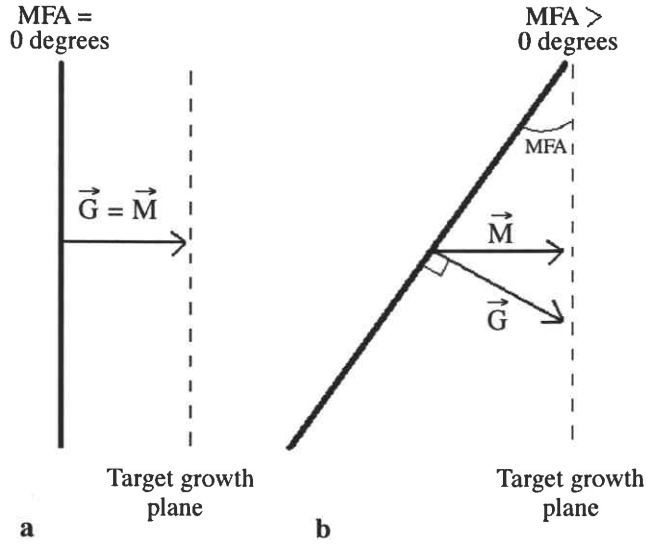

Figure 2. Theoretical growth showing the M vector, radial or tangential growth, and the G vector, growth of lignocellulosic matrix perpendicular to microfibril angle, for (**a**) zero microfibril angle and (**b**) some microfibril angle greater than 0 degrees. The target growth plane is assumed to parallel to the tracheid axis.

crystallites were assumed to stay constant at 35 Å (Fig. 1). The dimensions of the cellulose crystallites was kept constant while the lignin sheath thickness was allowed to vary as a function of microfibril angle (Fig. 1). The equation for this function is developed and demonstrated in Eq. 1 through 5. The S_1 and S_3 layer was assumed to be constant (Fig. 1).

Figures 2a & b demonstrate that a non-linear function was needed to explain the variation in microfibril angle as a function of lignin content. Various transformations of data were explored to determine the appropriate relationship in Figure 2 based on constraints defined in Figure 1. The exponential coefficient needed to transform the lignin data such that it linearly corresponded with microfibril angle was found.

It should be noted that, realistically, the polymer matrix does not grow to reach a certain plane. Instead, a fixed target plane was assumed to simulate how far the lignin matrix would have to develop for a higher microfibril angle to reach the same plane, an assumption needed since growth occurs perpendicular to the cellulose matrix (Gunning & Hardham 1982). Without such a constraint, and with the assumption of constant growth regardless of microfibril angle, one would expect lower growth rates in the radial direction for higher microfibril angles, which is not the case (Shupe *et al.* 1996a).

A power of 2 was used since the model was based on a two-dimensional plane (Fig. 2). The sum distance of lignin in the radial direction was computed through Figure 3. Figure 3 was derived by developing a spreadsheet that, through reiteration, computed the thickness of the lignin sheath based on varying lignin content. The spreadsheet was a mathematical linear model of Figure 1. It was also assumed that the middle lamella, lumen diameter, and cell wall thickness were constant. The range of lignin content for *P. palustris* was constrained to fall between 25 to 32 percent extractive free lignin content (including the middle lamella) (Koch 1972).

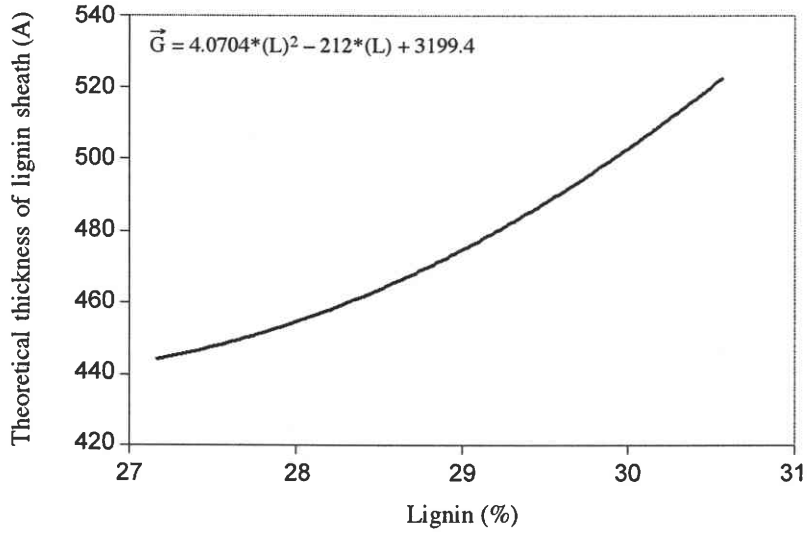

Figure 3. Theoretical sum thickness of lignin, in the radial or tangential direction, for a single microfibril within the S_2 layer. The non-linear equation derived from this figure was used for Equation 4.

Next, an equation using the power of 2 was derived. The coefficients were derived by setting constraints and then reiterating the squared equation with different coefficients until a specific coefficient yielded a minimum and maximum sum lignin sheath that equaled our estimates. That coefficient was then chosen for the 2-D plane equation (Eq. 1). The constraints set were as follows: the sum of the lignin sheath in the radial direction (Fig. 1) were: 439 Å (our computed equivalent to 25 % lignin) and 598 Å (our computed equivalent to 32 % lignin content). The equation was then solved such that when a 0° MFA was entered, the equation would yield the lower minimum of 439 Å while, when a 50° MFA was entered, the maximum of 598 Å would be the solution. In summary, the following constant and intercept was found such that the resulting range in $\vec{G}$ varied from 439 Å to 598 Å when the 2nd power was used (Fig. 2):

$$\vec{G} = 439 \text{ Å} + a\alpha^2 \quad (1)$$

Where a is some constant and α is microfibril angle. To determine the constant a, the following equation was solved:

$$598 \text{ Å} = 439 \text{ Å} + a(50°)^2 \quad (2)$$

The constant labeled "a" was found to be 0.0636. The following equation thus represented the sum thickness of the lignin sheath in the radial direction for Figure 1:

$$\vec{G} = 439 \text{ Å} + 0.0636*\alpha^2 \quad (3)$$

Next, a model to predict the sum thickness of the lignin sheath as a function of overall lignin percent was computed. The coefficients and intercept for the model were determined such that the range of $\vec{G}$ values fell between 439 to 598 Å and is presented in Figure 3:

$$\vec{G} = 4.0704*(L)^2 - 212*(L) + 3199.4 \quad (4)$$

Where L is lignin content percent. Eq. 3 was then set equal to Eq. 4 to yield the final equation:

$$\alpha = \sqrt{64*(L)^2 - 3333.3*(L) + 43402.52} \quad (5)$$

RESULTS

Trait variation within trees

Table 1 provides NIR models developed for extractives and lignin, which were in turn used to determine within tree variation of wood chemistry. X-ray diffraction was used to determine within tree variation of microfibril angle. Two wavelengths were found to best predict lignin while four wavelengths were needed for extractives.

Table 2 shows the within tree variation of lignin content. The mean lignin content was highest within the ring adjacent to the pith while just four years later, the lignin content commonly dropped by 1 to 2 percentage points. Lignin then continued to decline at a much slower rate from ring 4 to 16 resulting in only a 1 percentage point change. The overall range in lignin content from the wet lab chemistry analysis, and for all ages and heights combined, was 25 to 32 %. Table 2 gives an idea of where the high and low lignin contents reside within the tree. However, it should be noted that ring 1 was not included in the calibration due to the lack of wood volume needed to meet the

requirements of the standard (Tappi 1997, 1998). Nevertheless, since no samples at the pith were measured for wet lab chemistry due to a lack of adequate wood volume, a mild extrapolation in the equation was assumed to still adequately describe the ring 1 population. The extrapolation was considered mild since the variation in lignin at ring 5 was wide and the distribution incorporated three lignin values between 31 to 32%.

Table 1. Coefficients, R^2, and root mean square error of prediction for all models.

Model	Constants a	b	c	d	e	f	R^2	RMSEC
$\alpha = \sqrt{64*(L)^2 - 3333*(L) + 43403}$	-450	-8	40	3	–	–	0.40	9.80
$\alpha = a + b*(L)$	5.7	-143	–	–	–	–	0.40	9.35
NIR α[a] = 24.57 + a*(w1015[b]) + b*(1135) + c*(w1375) + d*(w1875) + c*(w1965) + f*(w2165)	1014	-314	-1552	626	-162	251	0.50	9.00
NIR E[c] = 2.27 + *a**(w1145) + *b**(1345) + *c**(w1685) + *d**(w2185)	408	-797	498	-134	–	–	0.71	3.27
NIR L = *a* + *b**(w1195) + *c**(w1015)	32	143	-201	–	–	–	0.55	2.13

a) NIR model for microfibril angle was only used to compare against theoretical model and not for within tree variation determination reported in Table 2 and 3.
b) For example, the absorbance at wavelength 1015 nm.
c) Where E represents extractives content.

Table 2. Experimental mean, standard deviation, and coefficient of variation for lignin for 10 trees at different height and ring numbers. N.A. represents no experimental data due to lack of material.

Tree height (m)	Extractive Free Wet Lab Klason Lignin % Ring number 1	4	8	16	32
4.6	30.4 07 (2.3%)	28.7 1.4 (4.8%)	28.4 1.1 (3.8%)	27.7 1.3 (4.5%)	27.3 1.5 (5.0%)
9.1	30.8 1.5 (4.7%)	28.8 1.1 (3.7%)	27.9 1.2 (4.3%)	27.5 1.3 (4.8%)	26.5 1.2 (3.9%)
13.7	30.4 2.0 (6.5%)	27.8 1.2 (4.3%)	27.8 1.4 (5.0%)	27.2 0.7 (2.4%)	26.6 1.0 (3.5%)
18.3	30.4 1.5 (4.9%)	28.5 0.6 (2.3%)	28.3 0.6 (2.1%)	27.9 1.1 (4.0%)	N.A.
22.9	28.6 1.9 (6.5%)	28.8 0.6 (1.9%)	28.4 0.9 (3.1%)	29.1 0.8 (2.6%)	N.A.
27.4	29.6 0.8 (2.8%)	30.1 1.7 (5.6%)	N.A.	N.A.	N.A.

Table 3. Experimental mean, standard deviation, and coefficient of variation for microfibril angle for 10 trees at different height and ring numbers. N.A. represents no experimental data due to lack of material.

Tree height (m)	Microfibril angle (°) Ring number 1	4	8	16	32
4.6	N.A.	40.3 6.3 (15.7%)	30.4 10.1 (33.2%)	15.2 8.5 (55.8%)	11.4 6.2 (54.3%)
9.1	N.A.	30.5 14.2 (46.7%)	17.7 8.3 (47.1%)	13.7 7.5 (54.8%)	10.4 7.9 (76.4%)
13.7	N.A.	24.8 5.3 (21.4%)	12.1 6.1 (50.1%)	11.1 5.2 (46.7%)	7.6 2.3 (30.5%)
18.3	N.A.	27.4 5.6 (20.1%)	16.3 5.9 (36.6%)	9.2 4.1 (44.7%)	N.A.
22.9	N.A.	31.7 5.9 (18.5%)	23.1 4.2 (18.2%)	15.1 7.4 (49.1%)	N.A.
27.4	N.A.	N.A.	N.A.	N.A.	N.A.

For most tree heights, there was no statistical difference between ring 16 and ring 32 (n=10). The exception was at a height between 22.9 to 27.4 m where inconsistent lignin patterns seemed to emerge (Table 2). Just about every ring and height category had similar coefficient of variation (COV) values with no specific patterns. In short, the age from the pith controlled the variation in lignin while the effect of tree height was negligible.

Table 3 shows microfibril angle variation throughout the tree. The range of the individual values, when estimating from the T-value, was between 4 and 55 degrees. A mean drop of 10° occurred between years 4 and 8 for most heights. At 4.6 m, a 15° drop occurred between years 8 and 16 while the difference was considerably lower at heights greater than 4.6 m. Microfibril angle continued to drop at a slower rate from 16 to 32 years of age for the lowest half of the tree while there was not enough material available to make a conclusion at greater tree heights. There was a distinct decrease in microfibril angle with a height up to 18.3 m and then the fibril angles either stabilized or increased. The variation in microfibril angle was great, particularly after ring 8. No difference in COV was detected between heights.

Table 4 shows the within tree toluene extractives variation. Extractive content decreased with age and height (Table 4). The highest extractive content occurred at ring 1 in the lower half of the tree while the lowest extractive content occurred at rings 16 and 32, regardless of height. The COV for extractive content was high and appeared to be attributable to within ring variation. The overall range in extractives content from the chemical analysis and for all ages and heights was 0 to 33%. Table 4 gives an idea of where the high and low extractives content reside within the tree. These patterns agree with Koch (1972) who also found extractives content to decrease from pith to bark for *P. palustris*. The heavy concentration of resin near the pith was probably attributable to an abundance of resin ducts that occur in the first few rings in southern pine (Larson *et al.* 2001).

Table 4. Experimental mean, standard deviation, and coefficient of variation for extractives for 10 trees at different height and ring numbers. N.A. represents no experimental data due to lack of material.

	Alcohol Toluene Wet Lab Extractives (%)				
Tree	Ring number				
height (m)	1	4	8	16	32
4.6	30.5 15.2 (49.9%)	17.7 13.9 (78.6%)	11.2 8.4 (74.9%)	3.7 1.8 (48.4%)	2.6 1.0 (54.3%)
9.1	27.3 14.9 (54.5%)	21.7 11.6 (54.2%)	8.3 7.2 (87.5%)	2.5 1.3 (54.3%)	2.0 0.9 (43.1%)
13.7	26.7 16.5 (61.8%)	13.4 5.2 (38.4%)	3.5 2.5 (70.7%)	2.5 0.90 (35.6%)	1.7 1.2 (73.4%)
18.3	18.8 7.2 (38.2%)	8.9 4.7 (52.5%)	3.3 1.2 (35.9%)	2.6 0.8 (31.7%)	2.4 1.2 (52.0%)
22.9	11.8 6.8 (57.4%)	4.6 1.3 (29.0%)	3.1 0.8 (24.1%)	2.4 0.5 (23.0%)	N.A.
27.4	6.0 1.0 (16.1%)	4.5 0.9 (20.4%)	N.A.	N.A.	N.A.

Lignin content to microfibril angle relationship

Figure 4 experimentally shows microfibril angle to increase with an increase in lignin content. When the residuals were investigated (not plotted), the variation in the residuals increased from 25 to 29 % lignin content and then stayed constant from 29 to 32 % lignin content. The R^2 (0.40) was not as high as that observed in a separate study where only the lignin in the S_2 layer was measured while that of the middle lamella was avoided (Table 1) (Gindl & Teischinger 2002; Gindl *et al.* 2004). The variation in mid-

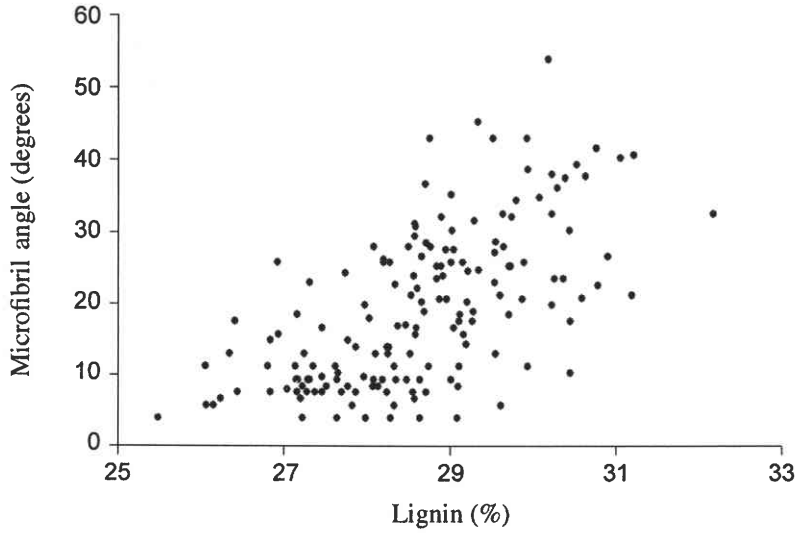

Figure 4. A scatter plot of experimental microfibril angle and lignin content.

dle lamella lignin composition probably added to the variation resulting in a decreased R^2 for this study. The RMSEC for the theoretical model was 9.8 while the empirical model was 9.35. Extractives content did not appear to influence the microfibril angle to lignin content relationship.

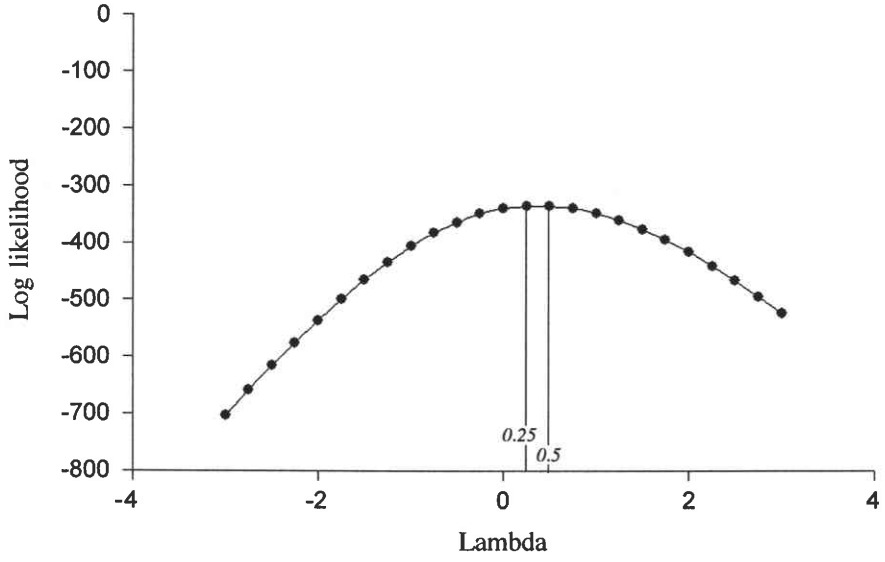

Figure 5. Log maximum likelihood results from Box-Cox transformation procedure with microfibril as the y variable and lignin % as the x variable.

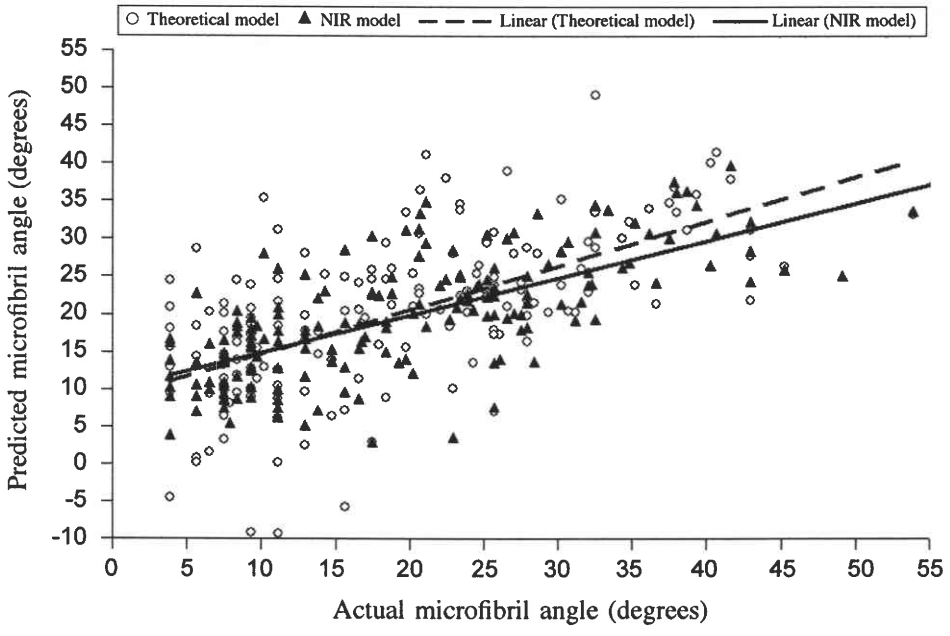

Figure 6. A scatter plot of predicted theoretical and predicted NIR model versus actual microfibril angle (derived from X-ray diffraction) for the theoretical and near infrared spectra model.

Figure 5 shows the log maximum likelihood results from 25 possible family of transformations using the Box-Cox method (Draper & Hunter 1969). The peak on Figure 4 represents the recommended statistical transformation by SAS (2001) that could be applied to lignin content when predicting microfibril angle and occurred at 0.5 which is the square root function, the same transformation as independently recommended in Equation 5.

An NIR absorbance model (NIR α^a) was constructed to predict microfibril angle from lignin content (Table 1). Six wavelengths from the near infrared region were needed to predict microfibril angle while the theoretical model (Eq. 5 and Table 1) needed only lignin content. Figure 6 shows a scatter plot comparing the capacity of using NIR absorbance and the theoretical model to predict lignin. The same samples used in Table 2 and 3 were used in the calibrations in Figure 6. There was no significant difference in slopes or intercepts when compared in only these two dimensions (Fig. 6). The two trendlines were almost parallel with a statistically insignificant crossover at around 15°. When the microfibril angle was predicted with both NIR and Eq. 5, a reasonable random scatter about the 1 : 1 line occurred, indicative that the two models were similar in prediction of microfibril angle. The relationship in Figure 7 supports that not only does microfibril angle relate to lignin by a growth function but, moreover, the microfibril angle as predicted by NIR is heavily dependent on lignin concentration.

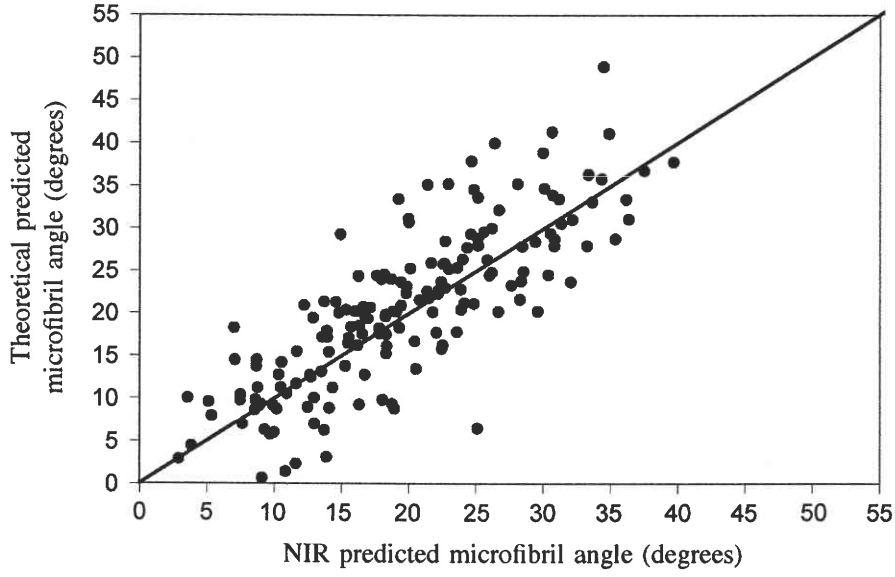

Figure 7. A scatter plot of NIR predicted microfibril angle versus the theoretically predicted microfibril angle ($R^2 = 0.65$).

DISCUSSION

Wood property variation

The mean lignin content was consistently higher than that reported for the innerwood and outerwood of loblolly pine (Table 2) (Shupe *et al.* 1996b; Shupe *et al.*1997). However, the results for this study were almost identical to those reported for *P. palustris*

where Koch (1972) found lignin to vary between 25 to 30%. Likewise, there did not appear to be any distinct effect of height on lignin. Such a result was notable since microfibril angle and extractives content showed distinct height differences but higher COVs. Since there was no apparent trend between height and lignin, but a trend did exist between microfibril angle and lignin (Table 2 & 3), one can conclude that some other unaccounted for variable drives the relationship between lignin and microfibril angle in the vertical direction. For this study, it was the variation in the radial direction of the tree in both lignin and microfibril angle that was important in the predictability of our model (Eq. 5).

The reason for such high variation in extractives content was due to within ring variation. Quite often, on solid wood pieces, a 10 mm interval within a ring would show distinct visual differences in color. These discolorations were not attributable to the proportion of latewood but were obvious resin pockets as deterimined by touch. The same samples, when ground up for wood chemistry, showed a characteristic dark color when compared to samples of much lower extractives content. When the spectra curve was analyzed at congruent regions, the spectra would drastically rise when the discolored brown areas were scanned. Likewise, the same visual change in color was observed in ground wood for equal density specimens, particularly in rings 1 and 4. A discolored brown tint occurred in rings 1 and 4 while samples further from the pith exhibited a light yellow shade. When the darker color was observed visually, the extractives content almost always measured in excess of 7% through wet lab chemistry (Tappi 1997, 1998). Such an impact on the spectra was important since NIR was used to predict lignin content and extractives will add error to the prediction of lignin (Soukupová *et al.* 2002).

The reason for the high variation in microfibril angle was less clear. Shupe *et al.* (1996a) showed COVs around 10% for both inner and outer wood of loblolly pine while for this study, the COVs ranged between 10 to 40%. However, the standard deviation in microfibril angle for this study averaged 6.7, while that for loblolly pine averaged 3 to 5 suggesting that the COVs should be carefully interpreted (Shupe *et al.* 1996a). It is noteworthy to mention that Shupe *et al.* (1996a) used a light microscope, which could avoid microfibril deviation near pit regions. However, it should also be noted that these samples were difficult to prepare to a uniform dimension due to the small radial widths of many latewood rings. This made acquisition of the T-value distribution more difficult.

As mentioned earlier, the axial or height variation in lignin was negligible, moderate for microfibril angle, and considerable for extractives. Both microfibril angle and extractives content decreased with tree height, when classified according to ring number from the pith. Such difference in properties between the top and bottom segments of the tree should disseminate an important point: the tree is a 3-dimensional structure with different multivariate properties in the vertical versus the radial direction. As a result, for the upper part of the stem, it may be incorrect to label the first few rings from the pith as juvenile wood since the microfibril angle and extractives content were lower than revealed in the core section of the butt log (Tables 2–4). Burdon *et al.* (2004) recently addressed this issue and recommended that the upper part of the stem not be classified as juvenile wood and instead developed a 2-dimensional categorization scheme. The

results of this study support Burdon *et al.* (2004) and, as such, it is recommended that juvenile wood should not be defined solely on the radial demarcation point of any one individual trait. Instead, one should consider the interaction of tree height by ring number and its effect on multiple traits when defining juvenile wood.

NIR lignin and extractives calibration models

The calibration of lignin and extractives from absorbance at selected NIR wavelengths resulted in a 0.55 and 0.71 R^2 respectively while the RMSEC for both were also high (Table 1). Schwanninger *et al.* (2004) suggest applying pretreatments to the spectra when calibrating for lignin. However, the low R^2 and high RMSEC for lignin was still present regardless of whether the raw, first, or second derivative data was used. Likewise, pretreatments such as multiplicative scatter correction and absorbance standardization did not significantly improve the R^2 or RMSEC in lignin calibration equations. Finally, partial least squares and principal components regression was also investigated to see if the predictive ability of lignin could be improved. It was found that 4 factors were needed for principal components and partial least squares regression to reach the same or better RMSEC and R^2 as when 2 independent variables were used in multiple linear regression. As such, multiple linear regression was used for lignin and extractives prediction. The competitive performance of multiple linear regression was perhaps attributable to the fact that the factors developed in principal components regression are based on all wavelengths while multiple linear regression just uses those of importance to the trait of interest (Via *et al.* 2003). A more detailed comparison of principal components and multiple linear regression for chemical and mechanical properties can be viewed in another paper in which the same calibration population, as in this study, was used to develop equations (Via *et al.* 2005). In that study, multiple linear regression was also found to sometimes be more robust than principal components regression. Wentzell and Montoto (2003) provide a detailed introduction and support that different multivariate calibration methods can be useful under different circumstances and that no specific calibration technique always provides superior predictive ability. Specifically, multiple linear regression, after careful selection of the independent variables, can provide similar predictive ability to partial least squares or principal components regression (Centner *et al.* 2000).

Since the RMSEC for lignin was still high after applying several spectral pretreatments and modeling methods, it was concluded that the majority of error embedded in the model was attributable to the sampling method. The main source of error was the location from which the spectra and wet lab chemistry was sampled. The lignin content was sampled throughout the entire cross section of the stem for a given ring while the spectra were only acquired at a single 5 mm diameter point (the radial face from an adjoining increment core). If we could have measured the microscale lignin in the same area (5 mm diameter) as spectra collection, lower RMSEC might be possible. Recent studies have indicated that wet lab measurement of lignin from just the 5 mm spot is possible and could improve the R^2 (Sykes *et al.* 2005). But despite this precision in wet lab chemistry, the prediction of lignin content through NIR can still be difficult (Sykes *et al.* 2005).

Another source of error was the large diameter spot size relative to the width of the latewood rings in the 30 plus rings from pith (a latewood ring was often less than 1 mm in width). Not only did this increase the error associated with predicting lignin, but it also influenced the absorbance since an increase in latewood mass will result in an increase in mean absorbance (Via *et al.* 2003). As such, any covariance present between latewood percent and lignin (Evans *et al.* 2000) would likewise influence the NIR calibration equation of both lignin and microfibril angle.

Additionally, the extractives content for *P. palustris* was high relative to other southern pines (Table 4). Such wide variation in extractives content probably lessened the ability to estimate lignin content due to the presence of phenolic compounds in both lignin and extractives. Soukupová *et al.* (2002) found the spectral features of lignin and soluble phenolics to be similar, resulting in a reduced ability to quantify lignin through NIR and consequently a lower R^2. Kelley and coworkers (2004b) also demonstrated that the precision to predict lignin decreased as the concentration of lignin decreased across a wide range of agricultural fibers. Despite the low R^2 between wet lab lignin and absorbance found in our study, it is possible the precision of the NIR instrument was higher than our wet lab chemistry (Foley *et al.* 1998). In order to achieve the type of accuracy exhibited by Foley *et al.* (1998), the accurate estimation of the slope between absorbance and lignin becomes important. Such a precise estimate of the slope is still possible if the full range of lignin and high sample size is pursued to counter the undesirable RMSEC. A high range in lignin was important because it provided increased leverage resulting in a more accurate slope (Neter *et al.* 1996). Likewise, the higher sample size ($n=70$) helped to provide a reasonable estimate of the mean response in lignin for a change in absorbance, despite the high RMSEC.

Finally, despite the fact that the variation in the signal increased as the wavelengths increased, the resultant signal to noise ratio still decreased with increasing wavelength. The resulting decrease in signal to noise ratio for the first overtone wavelengths were likely to influence our NIR calibration equation for lignin. Such a decrease in signal to noise ratio could result in models with higher RMSEC. However, in this study, the lower signal to noise ratio for the wavelengths used in calibration was offset by stronger p-values as determined through the Cp statistical selection method; where all possible combinations of wavelengths were considered (Via *et al.* 2005). As such, the absorbance at 1015 and 1195 nm wavelengths were used to calibrate for lignin content.

NIR and theoretical model of microfibril angle

The ability to model microfibril angle from lignin content (Eq. 5) was nearly as good as least squares regression for experimental data (Table 1). Eq. 5 slightly better accounted for the change in slopes with increasing lignin content, when compared to least squares regression, by applying the square root to the lignin side of the equation. Statistically, the Box Cox method also recommended the square root transformation which provided support for Eq. 5. Such a finding lends support for Eq. 5 since the theoretical model and hypothesis tests were developed *a priori*.

After the experiment was performed, new experimental evidence specific to the S_2 layer was published (Gindl *et al.* 2004). In that study, lignin content was found

to increase with increased microfibril angle; however, the variation in lignin was too great between 0 to 35 degrees to discern whether the relationship is linear or similar to Eq. 5. Nevertheless, when the compression wood microfibril angle and lignin data were omitted and the estimates (lignin estimated from graphs to ±1%) compared to the results of this study, Eq. 5 was statistically similar to coefficients developed from approximated data from Gindl *et al.* (2004) except for the intercept which was 4 degrees offset. The R^2 between lignin content and microfibril angle within the S_2 layer was much higher than our study since they were able to measure lignin and microfibril angle from the same tracheid and they were able to avoid any variation in lignin from the middle lamella, S_1, and S_3 (Gindl & Teischinger 2002; Gindl *et al.* 2004). Having a similar slope to their study was important since the R^2 between lignin and microfibril angle in our study was lower than their findings. Additionally, when their compression wood data was included (Gindl *et al.* 2004), Eq. 5 did not acceptably predict the shape of the curve supporting that Eq. 5 may not work under extrapolation conditions for compression wood samples. For our study, compression wood was avoided and was not accounted for in the theoretical model.

The theoretical model developed in Eq. 5 did not account for tree height. It should be noted that, in Tables 2 and 3, microfibril angle decreased with height up to 18.3 m while lignin content remained fairly stable suggesting that height played an additional role in the relation between lignin and microfibril angle. Height was not considered during our *a priori* theoretical model building stage.

An NIR absorbance model was also built in hopes of shedding light as to how NIR absorbance might correlate to microfibril angle. The NIR model had an RMSEC of only 0.80° lower than the theoretical model; yet, the NIR absorbance model relied on 6 independent variables compared to the one lignin variable in Eq. 5. However, since lignin was measured from two wavelengths (Table 1) then perhaps two independent variables were actually involved. Nevertheless, the lower number of variables was desirable and may result in a more robust model across populations, although that hypothesis would have to be tested. Additionally, it is important to point out that the signal to noise ratio was low for the wavelengths used in the NIR absorbance model and baseline shifts not attributable to lignin might add noise to the prediction.

The equal slope and intercept, as well as the fairly balanced residuals, support that NIR absorbance was apparently dependent on lignin content when used to predict microfibril angle. Schimleck and Evans (2002) found five wavelengths that were important in predicting microfibril angle, three of which were associated with cellulose. However, Schimleck and Evans (2002) also reported the 1510 and 2458 nm wavelengths to be important in predicting microfibril angle. While neither of these two wavelengths were used in our NIR absorbance models (Table 1), principal component regression loading on our data set showed these two wavelengths to be important in predicting microfibril angle. Additionally, lignin content and cellulose should be fairly collinear since they are measures of percent composition.

When using absorbance at NIR wavelengths to model microfibril angle, the RMSEC was high (9.0) when compared to other studies (1.8 to 2.0) (Schimleck & Evans 2002; Schimleck *et al.* 2003b). In these papers, partial least squares regression was used

which may sometimes account for lower RMSECs. However, our study differed in that we measured the absorbance matrix at rings 32. The rings this far from the pith were much narrower than the diameter of the NIR scan. Sometimes, as much as five rings were scanned when only a scan from one ring was desired. This was likely the source of additional RMSEC when compared to Schimleck's studies (Schimleck & Evans 2002; Schimleck *et al.* 2003b). Additionally, as mentioned earlier, the NIR spectra was acquired from one discrete spot while the wet lab chemistry was performed on the entire ring around the pith.

The theoretical equation suggested that the physical chemistry dimensions may change with a change in microfibril angle (Fig. 1). These end results agree with the Emons string model which also predicts an increase in microfibril angle with increased width of the microfibril although the mechanism is different and is analogous to wrapping a string around a tube (Emons *et al.* 2002).

Such a relationship between microfibril angle and lignin may be useful in genetics studies if lignin genetically covaries with microfibril angle. However, if a large environmental covariance between lignin and microfibril angle exist, then improper genetic analysis may occur. Pot *et al.* (2002) give an example of a genetic covariance matrix between wood chemistry and fiber morphology with the best scenario, for indirect selection of a trait, to be zero phenotypic correlation and strong genetic correlation. Similar exploration of the genetic covariance between wood lignin and microfibril angle is recommended before using NIR absorbance to estimate microfibril angle. Some tree improvement programs have already focused on decreasing lignin content by using NIR spectroscopy (Baillères *et al.* 2002; Yeh *et al.* 2004). In doing so, if genetically correlated, genetics programs may have also lowered microfibril angle.

Finally, more testing of Eq. 5 is recommended on more trees and at a single age to understand the level of predictability that occurs. Holding age constant can be important since different genes may be important at different ages in their effect on microfibril angle and lignin content response.

ACKNOWLEDGMENTS

This study was funded by the USDA National Research Initiative Competitive Grants Program Agreement No. 2001-35103-10908. This paper (No. 04-40-0317) is published with the approval of the Director of the Louisiana Agricultural Experiment Station. The authors would like to thank Dr. Ian Cave and David Jones for their critical review before submission.

REFERENCES

Baillères, H., F. Davrieux & F. Ham-Pichavant. 2002. Near infrared analysis as a tool for rapid screening of some major wood characteristics in a eucalyptus breeding program. Ann. For. Sci. 59: 479–490.

Brown, C.L. 1970. Physiology of wood formation in conifers. Wood Sci. 3: 8–22.

Burdon, R.D., R.P. Kibblewhite, J.C.F. Walker, R.A. Megraw, R. Evans & D.J. Cown. 2004. Juvenile versus mature wood: A new concept, orthogonal to corewood versus outerwood, with special reference to *Pinus radiata* and *P. taeda*. For. Sci. 50: 399–415.

Cave, I.D. 1966. Theory of X-ray diffraction method for the measurement of microfibril angle in wood. For. Prod. J. 16: 37–42.

Centner, V., J. Verdu-Andres, B. Walczak, D. Jouan-Rimbaud, F. Despagne, L. Pasti, D. Massart & O.E.D. Noord. 2000. Comparison of multivariate calibration techniques applied to experimental NIR data sets. Appl. Spec. 54: 608–623.

Donaldson, L.A. 1992. Within- and between-tree variation in microfibril angle in *Pinus radiata*. N.Z. J. For. Sci. 22: 77–86.

Donaldson, L.A. 2001. A three-dimensional computer model of the tracheid cell wall as a tool for interpretation of wood cell wall ultrastructure. IAWA J. 22: 213–233.

Draper, N.R. & W.G. Hunter. 1969. Transformations: some examples revisited. Technometrics 11: 23–40.

Emons, A.M.C., J.H.N. Schel & B.M. Mulder. 2002. The geometrical model for microfibril deposition and the influence of the cell wall matrix. Plant Biol. 4: 22–26.

Erickson, H.D. & T. Arima. 1974. Douglas-fir wood quality studies part II: effects of age and stimulated growth on fibril angle and chemical constituents. Wood Sci. Tech. 8: 255–265.

Evans, R., S. Stringer & R.P. Kibblewhite. 2000. Variation in microfibril angle, density and fibre orientation in twenty-nine *Eucalyptus nitens* trees. Appita J. 53: 450–457.

Fengel, D. 1970. Ultrastructural behavior of cell wall polysaccharides. Tappi J. 53: 497–503.

Foley, W.J., A. McIlwee, I. Lawler, L. Aragones, A.P. Woolnough, & N. Berding. 1998. Ecological applications of near infrared reflectance spectroscopy – a tool for rapid, cost-effective prediction of the composition of plant and animal tissues and aspects of animal performance. Oecologia 116: 293–305.

Gindl, W., M. Grabner & R. Wimmer. 2000. The influence of temperature on latewood lignin content in treeline Norway spruce compared with maximum density and ring width. Trees 14: 409–414.

Gindl, W., H.S. Gupta, T. Schöberl, H.C. Lichtenegger & P. Fratzl. 2004. Mechanical properties of spruce wood cell walls by nanoindentation. Applied Phys. A: Mat. Sci. Processing 79: 2069–2073.

Gindl, W. & A. Teischinger. 2002. Axial compression strength of Norway spruce related to structural variability and lignin content. Compos. A 33: 1623–1628.

Gindl, W., A. Teischinger, M. Schwanninger & B. Hinterstoisser. 2001. The relationship between near infrared spectra of radial wood surfaces and wood mechanical properties. J. Near Infrared Spectrosc. 9: 255–261.

Gunning, B.E.S. & A.R. Hardham. 1982. Microtubules. Ann. Rev. Plant Physiol. 33: 651–698.

Hepworth, D.G. & J.F.C. Vincent. 1998. Modeling the mechanical properties of xylem tissue from tobacco plants (*Nicotiana tabacum* 'Samsun') by considering the importance of molecular and micromechanisms. Ann. Bot. 81: 761–770.

Herman, M., P. Dutilleul & T. Avella-Shaw. 1999. Growth rate effects on *intra*-ring and *inter*-ring trajectories of microfibril angle in Norway spruce (*Picea abies*). IAWA J. 20: 3–21.

Heyn, A.N.J. 1969. The elementary fibril and supermolecular structure of cellulose in soft wood fiber. J. Ultra Res. . 26: 52–68.

Hoffmann, B., B. Chabbert, B. Monties & T. Speck. 2003. Mechancal, chemical and X-ray analysis of wood in the two tropical lianas *Bauhinia guianensis* and *Condylocarpon guianense*: variations during ontogeny. Planta 217: 32–40.

Jones, P.D., L.R. Schimleck, G.F. Peter, R.F. Daniels & A. Clark III. 2005. Nondestructive estimation of *Pinus taeda* L. wood properties for samples from a wide range of sites in Georgia. Can. J. For. Res. 35: 85–92.

Kelley, S.S., T.G. Rials, B. Snell, L.H. Groom & A. Sluter. 2004a. Use of near infrared spectroscopy to measure the chemical and mechanical properties of solid wood. Wood Sci. Tech. 38: 257–276.

Kelley, S.S., R.M. Rowell, M. Davis, C.K. Jurich & R. Ibach. 2004b. Rapid analysis of the chemical composition of agricultural fibers using near infared spectroscopy and pyrolysis molecular beam mass spectrometry. Biomass Bioenergy 27: 77–88.

Koch, P. 1972. Utilization of southern pines. Ag. Handbook 420: 188–189. USDA, Washington D.C., USA.

Köhler, L. & H.C. Spatz. 2002. Micromechanics of plant tissues beyond the linear-elastic range. Planta 215: 33–40.

Köhler, L., T. Speck & H. Spatz. 2000. Micromechanisms and anatomical changes during early ontogeny of two lianescent *Aristolochia* species. Planta 210: 691–700.

Larson, P.R. 1966. Changes in chemical composition of wood cell walls associated with age in *Pinus resinosa.* Forest Prod. J. 16: 37–45.

Larson, P.R., D.E. Kretschmann, A. Clark III & J.G. Isebrands. 2001. Formation and properties of juvenile wood in southern pines: a synopsis. Gen. Tech. Rep. FPL-GTR-129. 49 pp.

Lichtenegger, H., A. Reiterer, S.E. Stanzl-Tschegg & P. Fratzl. 1999. Variation of cellulose microfibril angles in softwoods and hardwoods – a possible strategy of mechanical optimization. J. Struct. Biol 128: 257–269.

Lindström, H., J.W. Evans & S.P. Verrill. 1998. Influence of cambial age and growth conditions on microfibril angle in young Norway spruce (*Picea abies* [L.] Karst.). Holzforschung 52: 573–581.

Lundgren, C. 2004. Microfibril angle and density patterns of fertilized and irrigated Norway spruce. Silva Fennica 38: 107–117.

McCann, M.C., N.J. Stacey, R. Wilson & K. Roberts. 1993. Orientation of macromolecules in the walls of elongating carrot cells. J. Cell Sci. 106: 1347–1356.

McMillin, C.W. 1973. Fibril angle of loblolly pine wood as related to specific gravity. Wood Sci. Tech. 2: 166–176.

Neter, J., M.H. Kutner, C.J. Nachtsheim & W. Wasserman. 1996. Applied linear statistical models. WCB McGraw-Hill, Boston, MA, USA. 1408 pp.

Nieduszy, I. & R.D. Preston. 1970. Crystallite size in natural cellulose. Nature 225: 273–274.

Peter, G.F., D.M. Benton & K. Bennett. 2003. A simple, direct method for measurement of microfibril angle in single fibres using differential interference contrast microscopy. J. Pulp Pap. Sci. 29: 274–280.

Poke, F.S., J.K. Wright & C.A. Raymond. 2004. Predicting extractives and lignin contents in *Eucalyptus globulus* using near infrared reflectance analysis. J. Wood Chem. Tech. 24: 55–67.

Pot, D., G. Chantre, P. Rozenberg, J.C. Rodrigues, G.L. Jones, H. Pereira, B. Hannrup, C. Caha lan & C. Plomion. 2002. Genetic control of pulp and timber properties in maritime pine (*Pinus pinaster* Ait.). Ann. For. Sci. 59: 563–575.

Reiterer, A., H. Lichtenegger, S. Tschegg & P. Fratzl. 1999. Experimental evidence for a mechanical function of the cellulose microfibril angle in wood cell walls. Philos. Mag. A 79: 2173–2184.

Saka, S. & M. Tsuji. 1987. The relationship between microfibril orientation in the tracheid S_2 layer and the lignin content of coniferous woods. Cell. Chem. Technol. 21: 225–231.

Sarén, M.P., R. Serimaa, S. Andersson, P. Saranpää, J. Keckes & P. Fratzl. 2004. Effect of growth rate on mean microfibril angle and cross-sectional shape of tracheids of Norway spruce. Trees 18: 354–362.

SAS – Statistical Analysis Software. 2001. Version 8.2. Cary, North Carolina, USA.

Schimleck, L. & R. Evans. 2002. Estimation of microfibril angle of increment cores by near infrared spectroscopy. IAWA J. 23: 225–234.

Schimleck, L., R. Evans & J. Ilic. 2001. Application of near infrared spectroscopy to a diverse range of species demonstrating wide density and stiffness variation. IAWA J. 22: 415–429.

Schimleck, L., R. Evans & J. Ilic. 2003b. Application of near infrared spectroscopy to the extracted wood of a diverse range of species. IAWA J. 24: 429–438.

Schimleck, L., R. Evans, D.P. Jones, R.F. Daniels, G.F. Peter & A. Clark. 2005. Estimation of microfibril angle and stiffness by near infrared spectroscopy using sample sets having limited wood density variation. IAWA J. 26: 175–187.

Schimleck, L., R. Evans & A.C. Matheson. 2002. Estimation of *Pinus radiata* D. Don clear wood properties by near-infrared spectroscopy. J. Wood Sci. 48: 132–137.

Schimleck L., C. Mora & R.F. Daniels. 2003a. Estimation of the physical wood properties of green *Pinus taeda* radial samples by near infrared spectroscopy. Can. J. For. Res. 33: 2297–2305.

Schimleck, L., R. Stürzenbecher, P.D. Jones & R. Evans. 2004. Development of wood property calibrations using near infrared spectra having different spectral resolutions. J. Near Infrared Spectrosc. 12: 55–61.

Schwanninger, M., B. Hinterstoisser, C. Gradinger, K. Messner & K. Fackler. 2004. Examination of spruce wood biodegraded by *Ceriporiopsis subvermispora* using near and mid infrared spectroscopy. J. Near Infrared Spectrosc. 12: 397–409.

Shupe, T.F., E.T. Choong, D.D. Stokke & M.D. Gibson. 1996a. Variation in cell dimensions and fibril angle for two fertilized even-aged loblolly pine plantations. Wood Fib. Sci. 28: 268–275.

Shupe, T.F., E.T. Choong & C.H. Yang. 1996b. The effects of silvicultural treatments on the chemical composition of plantation-grown loblolly pine wood. Wood Fib. Sci. 28: 295–300.

Shupe, T.F., C.Y. Hse, E.T. Choong & L.H. Groom. 1997. Differences in some chemical properties of innerwood and outerwood from five silviculturally different loblolly pine stands. Wood Fib. Sci. 29: 91–97.

Singh, A.P. & G. Daniel. 2001. The S_2 layer in the tracheid walls of *Picea abies* wood: inhomogeneity in lignin distribution and cell wall microstructure. Holzforschung 55: 373–378.

Soukupová, J., B.N. Rock & J. Albrechtová. 2002. Spectral characteristics of lignin and soluble phenolics in the near infrared – a comparative study. Int. J. Remote Sensing 23: 3039–3055.

Sykes, R., B. Li, G. Hodge, B. Goldfarb, J. Kadla & H. Chang. 2005. Prediction of loblolly pine wood properties using transmittance near-infrared spectroscopy. Can. J. For. Res. 35: 2423–2431.

Tappi Standard. 1997. Solvent extractives of wood and pulp. T 204 cm-97, Atlanta, GA, USA.

Tappi Standard. 1998. Acid-insoluable lignin in wood and pulp. T 222 om-98, Atlanta, GA, USA.

Taylor, J.G., T.P. Owen, L.T. Koonce & C.H. Haigler. 1992. Dispersed lignin in tracheary elements treated with cellulose synthesis inhibitors provides evidence that molecules of the secondary cell wall mediate wall patterning. Plant J. 2: 959–970.

Via, B.K., T.F. Shupe, L.H. Groom, M. Stine & C.L. So. 2003. Multivariate modeling of density, strength, and stiffness from near infrared spectra for mature, juvenile and pith wood of longleaf pine (*Pinus palustris*). J. Near Infrared Spectrosc. 11: 365–378.

Via, B.K., C.L. So, T.F. Shupe, L.G. Eckhardt, M. Stine & L.H. Groom. 2005. Prediction of wood mechanical and chemical properties in the presence and absence of blue stain using two infrared instruments. J. Near Infrared Spectrosc. 13: 201–212.

Wardrop, A.B. & H.E. Dadswell. 1955. The development of the conifer tracheid. Holzforschung 7: 33–39.

Wentzell, P.D. & L.V. Montoto. 2003. Comparison of principal components regression and partial least squares regression through generic simulations of complex mixtures. Chemometr. Int. Lab. Sys. 65: 257–279.

Wimmer, R., G.M. Downes & R. Evans. 2002. Temporal variation of microfibril angle in *Eucalyptus nitens* grown in different irrigation regimes. Tree Physiol. 22: 449–457.

Yeh, T.F., H.M. Chang & J.F. Kadla. 2004. Rapid prediction of solid wood lignin content using transmittance near-infrared spectroscopy. J. Agric. Food Chem. 52: 1435–1439.